Inverse Problems **38** (2022) 085008

UNIQUENESS THEOREMS FOR TOMOGRAPHIC PHASE RETRIEVAL WITH FEW CODED DIFFRACTION PATTERNS

ALBERT FANNJIANG

Abstract. 3D tomographic phase retrieval under the Born approximation for discrete objects supported on a $n\times n\times n$ grid is analyzed. It is proved that n projections are sufficient and necessary for unique determination by computed tomography (CT) with full projected field measurements and that $n+1$ coded projected diffraction patterns are sufficient for unique determination, up to a global phase factor, in tomographic phase retrieval. Hence $n+1$ is nearly, if not exactly, the minimum number of diffractions patterns needed for 3D tomographic phase retrieval under the Born approximation.

1. Introduction

Tomography is a commonly used method in a wide range of applications such as computed tomography [21], 3D diffractive imaging [7] and quantum state measurement [17].

Mathematically speaking, the forward model of tomography is based on various approximations of the nonlinear inverse scattering formulation (for example, the Lippmann-Schwinger integral equation). A simplification common to all current tomographic methods (except for geophysical applications) is based on either the Born or the Rytov approximation. The latter reduces to computed tomography (CT) in the limit of geometrical optics. The inversion methods of CT, which ignores the diffraction and scattering effects, have been well studied and documented [21]. On the other hand, the phase-unwrapping problem inherent to the Rytov approximation (see Section 2) is a largely unsolved problem and a major road block to its implementation [7].

An additional complication occurs in X-ray, optical scattering [2], electron diffraction [11, 12] as well as quantum state tomography [17], where only intensity measurements can be performed. This gives rise to the phase problem which requires phase retrieval techniques for solutions [10].

This brief note considers the imaging set-up based on the Born approximation where diffraction patterns (hence intensity-only measurements) in various directions are measured with a coded aperture and used to determine the 3D object (Figure 1).

In particular, we address the uniqueness question: Under what measurement schemes and with how many diffraction patterns, can one determine the 3D object uniquely (up to a global phase factor)?

To answer this question in a quantitative way, it is instructive (even imperative) to work with a discrete setting. After introducing the Born-projection approximation in Section 2 and laying out the discrete framework in Section 3, we recall some basic results about diffraction patterns in Section 4, in particular how the use of a random mask can improve

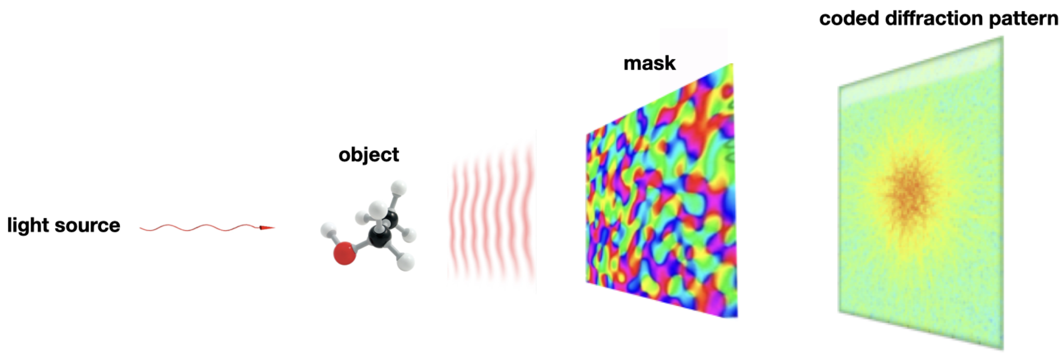

FIGURE 1. Diffraction pattern coded by a random mask placed behind the object. Different projections can be implemented by orientating the object in the corresponding direction, with the measurement set-up fixed. See, e.g. [19] for an similar experimental set-up

the quality of the measurement data (see also Remark 5.3). In Section 5 we first prove that with a random mask in the measurement of diffraction patterns, the tomographic phase retrieval problem reduces to that of CT modulo a simple ambiguity (Theorem 5.1). We then eliminate this ambiguity by deploying a sufficiently diverse set of $n+1$ projections under the prior constraint that the object does not become part of a line segment in any projection in the measurement scheme. As the uniqueness condition of n projections required for the standard CT (Theorem 5.5) sets a lower bound on the number of diffraction patterns for tomographic phase retrieval, the uniqueness condition of $n+1$ diffraction patterns (Theorem 5.8) is nearly optimal. We conclude with several remarks in Section 6.

2. Born and projection approximations

In scattering theory, the full field $u = u_i + u_s$ is written as the sum of the incident field u_i and the scattered field u_s. In the continuum setting, the full field $u(\mathbf{r})$ is governed by the Lippmann-Schwinger equation

$$u(\mathbf{r}) = u_i(\mathbf{r}) + \int d\mathbf{r}' G(\mathbf{r}-\mathbf{r}') f(\mathbf{r}') u(\mathbf{r}') \tag{1}$$

where f is the inhomogeneity, also called *scattering potential*, and G is the Green's function of the free-space Helmholtz equation [7].

Under the weak scatter assumption $|u_s| \ll |u_i|$, u in the (first-order) Born approximation is given by

$$u(\mathbf{r}) = u_i(\mathbf{r}) + \int d\mathbf{r}' G(\mathbf{r}-\mathbf{r}') f(\mathbf{r}') u_i(\mathbf{r}'). \tag{2}$$

Under the Fresnel approximation (with the z-axis as the optical axis, say),

$$G(\mathbf{r}) = \frac{-1}{4\pi} \frac{e^{\mathrm{i}\kappa|\mathbf{r}|}}{|\mathbf{r}|} \approx \frac{-1}{4\pi|z|} e^{\mathrm{i}\kappa|z|} e^{\mathrm{i}\frac{\kappa}{2}\frac{x^2+y^2}{|z|}} \tag{3}$$

and hence (2) becomes

$$u_i(\mathbf{r}) - \frac{e^{\mathrm{i}\kappa z}}{4\pi} \int dx'dy' \int dz' \frac{f(x',y',z')}{|z-z'|} e^{\mathrm{i}\frac{\kappa}{2}\frac{(x-x')^2+(y-y')^2}{|z-z'|}} e^{-\mathrm{i}\kappa z'} u_i(x',y',z'). \tag{4}$$

We think of the scattering process as consisting of two stages: First, the plane wave ($u_i(\mathbf{r}) = e^{\mathrm{i}\kappa z}$) illuminates and exits the scattering object; second, the exit wave transmits through a mask (located at $z = 0$) and propagates toward the detector.

In the first stage, consider the high Fresnel number regime

$$N_F = \frac{\ell^2}{\lambda z_0} \gg 1, \tag{5}$$

where ℓ is the typical size to be resolved, λ the wavelength and z_0 the thickness of the object. In this limit (5),

$$\frac{-\mathrm{i}\kappa}{2\pi|z-z'|} e^{\mathrm{i}\frac{\kappa}{2}\frac{(x-x')^2+(y-y')^2}{|z-z'|}} \longrightarrow \delta(x-x', y-y'), \quad \text{as } N_F \to \infty$$

for all $z \neq z'$, the exit wave (4) at $z = 0$ is approximated by

$$v_B(x,y) = 1 - \frac{\mathrm{i}}{2\kappa} \int dz' f(x,y,z'). \tag{6}$$

The right hand side of (6) is the *projection approximation* under the first-order Born assumption. On the other hand, the exit wave with the Rytov approximation is given by

$$v_R(x,y) = \exp\left[-\frac{\mathrm{i}}{2\kappa} \int dz' f(x,y,z')\right].$$

Since

$$v_B - 1 = \ln v_R \mod 2\pi\mathrm{i}, \tag{7}$$

the Born scattered field is the unwrapped phase of the Rytov approximation.

In short, the Born-projection approximation is the linear approximation of the Rytov-projection approximation and both approximations employ the projection approximation [6].

The projection approximation corresponds to light propagation through the scatterer in parallel straight lines. Its validity, however, depends on the spatial resolution of the imaging system as follows.

Radiation of wavelength λ scattered by features of size ℓ, that are to be resolved, would have a maximum diffraction angle of the order of $\Delta\theta = \lambda/\ell$. Hence the maximum spread of the radiation at the exit plane would be $\Delta\theta z_0$ where z_0 is the thickness of the sample. The projection approximation is valid if the spread is much smaller than the resolution, i.e.

$$\lambda z_0/\ell \ll \ell. \tag{8}$$

which is exactly equivalent to the high Fresnel number regime (5) [22].

At the second stage, the exit wave v_B is first multiplied by the mask function μ and then propagates into the far-field as $\mathcal{F}(\mu\cdot v_B)$ where $\mathcal{F}$ is the Fourier transform in the transverse variables. The measured coded diffraction pattern $|\mathcal{F}(\mu\cdot v_B)|^2$ is given by

$$|\mathcal{F}(\mu\cdot v_B)|^2 \quad = \quad |\mathcal{F}(\mu)|^2+\frac{1}{\kappa}\Im\{\overline{\mathcal{F}\mu}\cdot\mathcal{F}(\mu\int f dz')\}+\frac{1}{4\kappa^2}|\mathcal{F}(\mu\int f dz')|^2 \tag{9}$$

where $\Im$ denotes the imaginary part. This technique, with or without coded aperture, is sometimes called the *propagation-based phase contrast* method [22].

Tomographic microscopy based on the linear forward model ignoring the nonlinear term $|\mathcal{F}(\mu\int dz' f)|^2$ on the right hand side of (9) is a form of bright-field imaging (see [18, 23]). As (9) represents the interference pattern between the reference wave $\mathcal{F}(\mu)$ and the masked object wave $-\mathrm{i}\mathcal{F}(\mu\int f dz')/(2\kappa)$, reconstruction from the linear term in (9) can be performed by conventional holographic techniques [25, 26].

Adopting the dark-field mode of imaging (see [15] where the pupil or probe function plays the role of coded aperture), we focus on the more challenging nonlinear term as the measurement data and analyze the inherent information content therein. The nonlinear effect of a coded aperture is a key ingredient of our set-up. The next key ingredient to an information-based approach is discretization.

3. Discrete tomography

To motivate the discrete setup, consider the continuum setting. It is a classical result that a compactly supported function on, e.g. the cube, is uniquely determined by the Fourier transform (magnitude & phase) in any infinite set of projections ([14], Proposition 7.8) while for any finite set of projections, counterexamples to unique determination can be constructed ([14], Proposition 7.9).

As a consequence, uniqueness with Fourier *intensity* data in the continuum setting would require additional assumptions besides an infinite number of projections. It is not currently known, however, what additional assumptions are needed to guarantee uniqueness with intensity-only measurements.

Working with a discrete set-up we aim to derive a quantitative, information-based theory of uniqueness. To this end, we adopt the framework of [1] whose main advantage is preserving the fundamental Fourier slice theorem (Theorem 3.1).

For simplicity, we choose the physical units so that $\kappa = 2\pi$. Let $[\![k, l]\!]$ denote the integers between and including the integers k and l. We define a 3D $n\times n\times n$ object as the set

$$f = \{f(i, j, k)\in\mathbb{C} : i, j, k\in\mathbb{Z}_n\} \tag{10}$$

where

$$\mathbb{Z}_n \quad = \quad \begin{cases} [\![-n/2, n/2-1]\!] & \text{if } n \text{ is an even integer;}\\ [\![-(n-1)/2, (n-1)/2]\!] & \text{if } n \text{ is an odd integer.}\end{cases} \tag{11}$$

We define three families of line segments, the x-lines, y-lines, and z-lines. Formally, a x-line, denoted by $\ell_{x(\alpha,\beta)}(c_1, c_2)$, is defined as

$$\ell_{x(\alpha,\beta)}(c_1, c_2) : \begin{bmatrix} y \\ z \end{bmatrix} = \begin{bmatrix} \alpha x + c_1 \\ \beta x + c_2 \end{bmatrix} \qquad c_1, c_2 \in \mathbb{Z}_{2n-1}, \quad x \in \mathbb{Z}_n \tag{12}$$

To avoid wraparound of x-lines with $|\alpha|, |\beta| \leq 1$, we can zero-pad f in a larger lattice $\mathbb{Z}_p^3$ with $p \geq 2n-1$. This is particularly important when it comes to define the X-ray transform by a line sum (cf. (18)-(20)) without wrapping around the object domain.

Similarly, a y-line and a z-line are defined as

$$\ell_{y(\alpha,\beta)}(c_1, c_2) : \begin{bmatrix} x \\ z \end{bmatrix} = \begin{bmatrix} \alpha y + c_1 \\ \beta y + c_2 \end{bmatrix} \qquad c_1, c_2 \in \mathbb{Z}_{2n-1}, \quad y \in \mathbb{Z}_n, \tag{13}$$

$$\ell_{z(\alpha,\beta)}(c_1, c_2) : \begin{bmatrix} x \\ y \end{bmatrix} = \begin{bmatrix} \alpha z + c_1 \\ \beta z + c_2 \end{bmatrix} \qquad c_1, c_2 \in \mathbb{Z}_{2n-1}, \quad z \in \mathbb{Z}_n. \tag{14}$$

We denote the sets of all x-lines, y-lines, and z-lines by $\mathcal{L}_x, \mathcal{L}_y$, and $\mathcal{L}_z$, respectively.

Also, we denote the family of lines that corresponds to a fixed pair (α, β) and variable intercepts (c_1, c_2) by $\ell_{x(\alpha,\beta)}, \ell_{y(\alpha,\beta)}$ and $\ell_{z(\alpha,\beta)}$ for a family of parallel x-lines, y-lines, and z-lines, respectively. Note that $\ell_{x(1,\beta)} = \ell_{y(1,\beta)}, \ell_{x(\alpha,1)} = \ell_{z(1,\alpha)}$ and $\ell_{y(\alpha,1)} = \ell_{z(\alpha,1)}$.

Let f_x be the continuous interpolation of f in the directions perpendicular to x as follows:

$$f_x(i, y, z) = \sum_{j \in \mathbb{Z}_n} \sum_{k \in \mathbb{Z}_n} f(i, j, k) D_p(y - j) D_p(z - k), \quad y, z \in \mathbb{R} \tag{15}$$

where D_p is the p-periodic Dirichlet kernel given by

$$D_p(t) = \frac{1}{p} \sum_{l \in \mathbb{Z}_p} e^{\mathrm{i}2\pi lt/p} = \begin{cases} 1, & t = mp, \quad m \in \mathbb{Z} \\ \frac{\sin(\pi t)}{p \sin(\pi t/p)}, & \text{else.} \end{cases}$$

In particular, $D_p(t) = 0$ for $t \in \mathbb{Z}/\mathbb{Z}_p$, i.e. $[D_p(i-j)]_{i,j \in \mathbb{Z}_p}$ is the $p \times p$ identity matrix.

Similarly we define the interpolation of f perpendicular to y and z, respectively, as

$$f_y(x, j, z) = \sum_{i \in \mathbb{Z}_n} \sum_{k \in \mathbb{Z}_n} f(i, j, k) D_p(x - i) D_p(z - k), \quad x, z \in \mathbb{R}; \tag{16}$$

$$f_z(x, y, k) = \sum_{i \in \mathbb{Z}_n} \sum_{j \in \mathbb{Z}_n} f(i, j, k) D_p(x - i) D_p(y - j), \quad x, y \in \mathbb{R}. \tag{17}$$

By interpolating from the grid points (15)-(17), we have extended f from $\mathbb{Z}_p^3$ to the hyperplanes $x = i$, $y = j$ or $z = k$, where $i, j, k \in \mathbb{Z}_p$.

The main, and only, purpose for interpolating the discrete object is to make possible the definition of a diversified set of the discrete X-ray transforms. Having extended the domain of f to the hyperplanes $x = i$, $y = j$ or $z = k$, where $i, j, k \in \mathbb{Z}_{2n-1}$, we define the discrete

X-ray transforms as the line sums

$$f_{x(\alpha,\beta)}(c_1,c_2) = \sum_{i\in\mathbb{Z}_n} f_x(i,\alpha i+c_1,\beta i+c_2), \tag{18}$$

$$f_{y(\alpha,\beta)}(c_1,c_2) = \sum_{j\in\mathbb{Z}_n} f_y(\alpha j+c_1,j,\beta j+c_2) \tag{19}$$

$$f_{z(\alpha,\beta)}(c_1,c_2) = \sum_{k\in\mathbb{Z}_n} f_z(\alpha k+c_1,\beta k+c_2,k) \tag{20}$$

with $c_1, c_2 \in \mathbb{Z}_{2n-1}$. With zero-padding, we take $\mathbb{Z}_p^2$, $p \geq 2n-1$, as the domain of the X-ray transforms.

Without the interpolation (15)-(17), the discrete X-ray transforms are not well-defined except for $(\alpha,\beta) = (\pm 1, 0), (0, \pm 1), (\pm 1, \pm 1)$. For simplicity of terminology, we shall refer to X-ray transforms simply as *projections*.

The 3D Fourier transform $\widehat{f}$ of the object f, supported in $\mathbb{Z}_n^3 \subset \mathbb{Z}_p^3$, is given by

$$\widehat{f}(\xi,\eta,\zeta) = \sum_{i,j,k\in\mathbb{Z}_n} f(i,j,k)e^{-\mathrm{i}2\pi(\xi i+\eta j+\zeta k)/p}. \tag{21}$$

Note that $\widehat{f}$ in (21) is a p-periodic function band-limited to $\mathbb{Z}_n^3$. The associated 1-D and 2-D (partial) Fourier transforms are similarly defined p-periodic band-limited functions.

The Fourier slice theorem concerns the 2-D discrete Fourier transform $\widehat{f_x}(\alpha,\beta)$, defined as

$$\widehat{f}_{x(\alpha,\beta)}(\eta,\zeta) = \sum_{j,k\in\mathbb{Z}_n} f_{x(\alpha,\beta)}(j,k)e^{-\mathrm{i}2\pi(\eta j+\zeta k)/p} \tag{22}$$

and the 3-D discrete Fourier transform given in (21).

The following Fourier slice theorem resembles that of the continuous case [21] and plays a central role in the framework of discrete tomography.

Theorem 3.1. *[1] (Fourier slice theorem) For a given family of x-lines $\ell_x(\alpha,\beta)$ with fixed slopes (α,β) and variable intercepts (c_1,c_2). Then the 2D discrete Fourier transform $\widehat{f}_{x(\alpha,\beta)}$ of the x-projection $f_{x(\alpha,\beta)}$ and the 3D discrete Fourier transform $\widehat{f}$ of the object f satisfy the equation*

$$\widehat{f}_{x(\alpha,\beta)}(\eta,\zeta) = \widehat{f}(-\alpha\eta-\beta\zeta,\eta,\zeta). \tag{23}$$

Likewise, we have

$$\widehat{f}_{y(\alpha,\beta)}(\xi,\zeta) = \widehat{f}(\xi,-\alpha\xi-\beta\zeta,\zeta), \tag{24}$$

$$\widehat{f}_{z(\alpha,\beta)}(\xi,\eta) = \widehat{f}(\xi,\eta,-\alpha\xi-\beta\eta). \tag{25}$$

3.1. **Continuum limit.** One can justify the above discrete framework, especially the interpolation scheme (15)-(17) and the related line average (18)-(20), from the perspective of continuum limit.

Suppose the discrete object f above is the restriction of some smooth function f_* supported on $[-1/2, 1/2]^3$ in the sense that

$$f(i,j,k) = f_*\Big(\frac{i}{n}, \frac{j}{n}, \frac{k}{n}\Big)$$

or some local average of f_* about each grid point. As $p \to \infty$, the Dirichlet kernel has the limit

$$\lim_{p\to\infty} pD_p(pt) = \delta(t),$$

Dirac's delta function. For a sufficiently smooth f_*, the right hand side of (15), after proper normalization, approaches the limit

$$\int f_*(x, y', z')\delta(y - y')\delta(z - z')dy'dz' \quad = \quad f_*(x, y, z)$$

In other words, the interpolation becomes exactly an identity in the continuum limit. Likewise, the discrete X-ray transforms (18)-(20), after proper normalization, become line integrals (i.e. the continuous X-ray transforms).

Finally, in the continuum limit, Theorem 3.1 gives rise to the standard Fourier slice theorem. In other words, the discrete framework is a structure-preserving discretization of the continuous setting.

4. Diffraction patterns

For ease of notation, we denote by $\mathbf{t}$ the direction of projection, $x(\alpha, \beta), y(\alpha, \beta)$ or $z(\alpha, \beta)$. Let $\mathcal{T}$ denote the set of directions $\mathbf{t}$ employed in the tomographic measurement. Let $p = 2n - 1$.

Let the Fourier transform of the projection $f_\mathbf{t}$ be written as

$$F_\mathbf{t}(e^{-\mathrm{i}2\pi\mathbf{w}}) = \sum_{\mathbf{n}\in\mathbb{Z}_p^2} e^{-\mathrm{i}2\pi\mathbf{n}\cdot\mathbf{w}} f_\mathbf{t}(\mathbf{n}), \quad \mathbf{w} \in \Big[-\frac{1}{2}, \frac{1}{2}\Big]^2,$$

where $f_\mathbf{t}$ vanishes outside $\mathbb{Z}_n^2$. In the absence of a random mask ($\mu \equiv 1$), the continuous diffraction pattern in the far field can be written as

$$|F_\mathbf{t}(e^{-\mathrm{i}2\pi\mathbf{w}})|^2 = \sum_{\mathbf{n}\in\mathbb{Z}_{2p-1}^2} \left\{ \sum_{\mathbf{n}'\in\mathbb{Z}_p^2} f_\mathbf{t}(\mathbf{n}' + \mathbf{n})\overline{f_\mathbf{t}(\mathbf{n}')} \right\} e^{-\mathrm{i}2\pi\mathbf{n}\cdot\mathbf{w}}, \quad \mathbf{w} \in \Big[-\frac{1}{2}, \frac{1}{2}\Big]^2, \tag{26}$$

[8]. Here and below the over-line notation means complex conjugacy. The expression in the brackets in (26) is the autocorrelation function of $f_\mathbf{t}$.

The diffraction patterns are then uniquely determined by sampling on the grid

$$\mathbf{w} \in \frac{1}{2p-1}\mathbb{Z}_{2p-1}^2 \tag{27}$$

or by Kadec's 1/4-theorem on any following irregular grid [27]

$$\{\mathbf{w}_{jk},\ j, k \in \mathbb{Z}_{2p-1} : |(2p-1)\mathbf{w}_{jk} - (j, k)| < 1/4\}. \tag{28}$$

With the Nyquist, regular (27) or irregular (28), sampling, the diffraction pattern contains the same information as does the autocorrelation function of $f_{\mathbf{t}}$.

4.1. **Inherent ambiguities.** The following standard result explicates all the ambiguities corresponding to the same diffraction pattern.

Proposition 4.1. *[13] Let the z-transform $F_{\mathbf{t}}(\mathbf{z}) = \sum_{\mathbf{n}\in\mathbb{Z}_p^2} f_{\mathbf{t}}(\mathbf{n})\mathbf{z}^{-\mathbf{n}}$ be given by*

$$F_{\mathbf{t}}(\mathbf{z}) = \alpha \mathbf{z}^{-\mathbf{m}} \prod_{k=1}^{q} F_k(\mathbf{z}), \quad \mathbf{m} \in \mathbb{N}^2, \quad \alpha \in \mathbb{C} \tag{29}$$

where $F_k, k = 1, \ldots, q$, are non-monomial irreducible polynomials. Let $G_{\mathbf{t}}(\mathbf{z})$ be the $\mathbf{z}$-transform of another finite array $g_{\mathbf{t}}(\mathbf{n})$. Suppose $|F_{\mathbf{t}}(e^{-\mathrm{i}2\pi\mathbf{w}})| = |G_{\mathbf{t}}(e^{-\mathrm{i}2\pi\mathbf{w}})|, \forall \mathbf{w} \in [0,1]^2$. Then

$$G_{\mathbf{t}}(\mathbf{z}) = |\alpha| e^{\mathrm{i}\theta} \mathbf{z}^{-\mathbf{q}} \left(\prod_{k\in I} F_k(\mathbf{z})\right) \left(\prod_{k\in I^c} \overline{F_k(1/\bar{\mathbf{z}})}\right), \quad \textit{for some} \quad \mathbf{q} \in \mathbb{N}^2, \theta \in \mathbb{R}, \tag{30}$$

where I is a subset of $\{1, 2, \ldots, q\}$.

Remark 4.2. *The undetermined monomial factor $\mathbf{z}^{-\mathbf{q}}$ in (30) corresponds to the translation invariance of the Fourier intensity data while the altered factors $\overline{F_k(1/\bar{\mathbf{z}})}$ corresponds to the conjugate inversion invariance of the Fourier intensity data (see Corollary 4.4 below). The conjugate inversion of $f_{\mathbf{t}}$, called the twin image, is defined by $\mathrm{Twin}(f_{\mathbf{t}})(\mathbf{n}) = \bar{f}_{\mathbf{t}}(-\mathbf{n})$.*

Next consider a random mask $\mu(\mathbf{n}) = e^{\mathrm{i}\phi(\mathbf{n})}$ where $\phi(\mathbf{n})$ are independent, continuous random variables over $[-\pi, \pi)$. To fix the idea, let the mask be placed between the object and the detectors (Figure 1) so that the measured diffraction pattern is the intensities of the Fourier transform of the masked projection $\widetilde{f}_{\mathbf{t}}(\mathbf{n}) = f_{\mathbf{t}}(\mathbf{n})\mu(\mathbf{n})$, i.e. the μ-coded diffraction pattern.

Let $f_{\mathbf{t}}$ be not part of a line object. An object is part of a line object if its support is a subset of a line. Consequently, the masked projection $\widetilde{f}_{\mathbf{t}}(\mathbf{n})$ is not part of a line object.

Recall [8] that the $z-$transform of the non-line masked object projection is irreducible, up to a monomial as stated below.

Proposition 4.3. *[8] Suppose $f_{\mathbf{t}}$ is not a line object and let μ be the phase mask with phase at each point continuously and independently distributed over $[-\pi, \pi)$. Then with probability one the z-transform of the masked object $\widetilde{f}_{\mathbf{t}} = f_{\mathbf{t}} \odot \mu$ does not have any non-monomial irreducible polynomial factor.*

The masked object is also called the *exit wave* in the parlance of optics literature. In other words, a coded diffraction pattern is just the plain diffraction pattern of a masked object.

The following corollary will be useful for subsequent analysis.

Corollary 4.4. *Under the assumptions of Proposition 4.3, if another masked object projection* $\widetilde{g}_{\mathbf{t}} := \nu g_{\mathbf{t}}$ *produces the same diffraction pattern as* $\widetilde{f}_{\mathbf{t}} = \mu \odot f_{\mathbf{t}}$*, then for some* $\mathbf{p}$ *and* θ

$$\widetilde{f}_{\mathbf{t}}(\mathbf{n}+\mathbf{p}) \quad = \quad e^{-\mathrm{i}\theta}\widetilde{g}_{\mathbf{t}}(\mathbf{n}) \quad \text{or} \quad e^{\mathrm{i}\theta}\,\mathrm{Twin}(\widetilde{g}_{\mathbf{t}})(\mathbf{n}) \tag{31}$$

for all $\mathbf{n}$.

Proof. Let $\widetilde{F}_{\mathbf{t}}$ and $\widetilde{G}_{\mathbf{t}}$ be the z-transforms of $\widetilde{f}_{\mathbf{t}}$ and $\widetilde{g}_{\mathbf{t}}$, respectively. By Proposition 4.3 and (30),

$$\widetilde{G}_{\mathbf{t}}(\mathbf{z}) = e^{\mathrm{i}\theta}\mathbf{z}^{-\mathbf{p}}\widetilde{F}_{\mathbf{t}}(\mathbf{z}) \quad \text{or} \quad e^{\mathrm{i}\theta}\mathbf{z}^{-\mathbf{p}}\overline{\widetilde{F}_{\mathbf{t}}(1/\bar{\mathbf{z}})}, \quad \text{for some } \mathbf{p},\ \theta \text{ and all } \mathbf{z}.$$

which after substituting $\mathbf{z} = \exp(-\mathrm{i}2\pi\mathbf{w})$ becomes

$$\widetilde{G}_{\mathbf{t}}(e^{-\mathrm{i}2\pi\mathbf{w}}) = e^{\mathrm{i}\theta}e^{\mathrm{i}\mathbf{w}\cdot\mathbf{p}}\widetilde{F}_{\mathbf{t}}(e^{-\mathrm{i}2\pi\mathbf{w}}) \quad \text{or} \quad e^{\mathrm{i}\theta}e^{\mathrm{i}\mathbf{w}\cdot\mathbf{p}}\overline{\widetilde{F}_{\mathbf{t}}(e^{-\mathrm{i}2\pi\mathbf{w}})}, \quad \text{for some } \mathbf{p},\ \theta \text{ and all } \mathbf{z}.$$

Note that $\widetilde{G}_{\mathbf{t}}(e^{-\mathrm{i}2\pi\mathbf{w}})$ and $\widetilde{F}_{\mathbf{t}}(e^{-\mathrm{i}2\pi\mathbf{w}})$ are the Fourier transforms of $\widetilde{g}_{\mathbf{t}}$ and $\widetilde{f}_{\mathbf{t}}$, respectively. Therefore in view of Remark 4.2 we have

$$\widetilde{g}_{\mathbf{t}}(\mathbf{n}) \quad = \quad e^{\mathrm{i}\theta}\widetilde{f}_{\mathbf{t}}(\mathbf{n}-\mathbf{p}) \quad \text{or} \quad e^{\mathrm{i}\theta}\,\mathrm{Twin}(\widetilde{f}_{\mathbf{t}})(\mathbf{n}-\mathbf{p}),$$

which is equivalent to (31). □

By Corollary 4.4, for some $\mathbf{m}_{\mathbf{t}} \in \mathbb{Z}^2, \theta_{\mathbf{t}} \in \mathbb{R}$, we have

$$\begin{aligned} g_{\mathbf{t}}(\mathbf{n})\nu(\mathbf{n}) \quad &= \quad e^{\mathrm{i}\theta_{\mathbf{t}}} f_{\mathbf{t}}(\mathbf{n}+\mathbf{m}_{\mathbf{t}})\mu(\mathbf{n}+\mathbf{m}_{\mathbf{t}}) \\ \text{or} \quad \mathrm{Twin}(g_{\mathbf{t}}\nu)(\mathbf{n}) \quad &= \quad e^{-\mathrm{i}\theta_{\mathbf{t}}} f_{\mathbf{t}}(\mathbf{n}+\mathbf{m}_{\mathbf{t}})\mu(\mathbf{n}+\mathbf{m}_{\mathbf{t}}). \end{aligned} \tag{32}$$

Since $\mathrm{Twin}(g_{\mathbf{t}})(\mathbf{n}) = \bar{g}_{\mathbf{t}}(-\mathbf{n})$, we rewrite (32) as

$$g_{\mathbf{t}}(\mathbf{n})\nu(\mathbf{n}) \quad = \quad \begin{cases} e^{\mathrm{i}\theta_{\mathbf{t}}} f_{\mathbf{t}}(\mathbf{n}+\mathbf{m}_{\mathbf{t}})\mu(\mathbf{n}+\mathbf{m}_{\mathbf{t}}) \\ e^{\mathrm{i}\theta_{\mathbf{t}}} \bar{f}_{\mathbf{t}}(-\mathbf{n}+\mathbf{m}_{\mathbf{t}})\bar{\mu}(-\mathbf{n}+\mathbf{m}_{\mathbf{t}}) \end{cases} \tag{33}$$

If μ is completely known, i.e. $\nu = \mu$, then (33) becomes

$$g_{\mathbf{t}}(\mathbf{n})\mu(\mathbf{n}) \quad = \quad \begin{cases} e^{\mathrm{i}\theta_{\mathbf{t}}} f_{\mathbf{t}}(\mathbf{n}+\mathbf{m}_{\mathbf{t}})\mu(\mathbf{n}+\mathbf{m}_{\mathbf{t}}) \\ e^{\mathrm{i}\theta_{\mathbf{t}}} \bar{f}_{\mathbf{t}}(-\mathbf{n}+\mathbf{m}_{\mathbf{t}})\bar{\mu}(-\mathbf{n}+\mathbf{m}_{\mathbf{t}}). \end{cases} \tag{34}$$

Our goal is to prove that with a sufficiently large $\mathcal{T}$, (33) yields $g = f$ and $\mu = \nu$, up to a constant phase factor, almost surely, i.e. $\mathbf{m}_{\mathbf{t}} = 0$ and $\theta_{\mathbf{t}} = \text{const.}$ for all $\mathbf{t}$ and eventually design an efficient algorithm to reconstruct f.

5. Uniqueness theorems

Our first main result is that with the help of a random mask, tomographic phase retrieval reduces to computed tomography modulo the ambiguity that the object projection is independent of the direction used in the measurement scheme.

Theorem 5.1 (Reduction to CT modulo an ambiguity)**.** *Consider a random phase mask* $\mu(\mathbf{n}) = \exp[\mathrm{i}\phi(\mathbf{n})]$ *with independent, continuous random variables* $\phi(\mathbf{n}) \in \mathbb{R}$*. Suppose that* $f_{\mathbf{t}}$ *is a non-line object for all* $\mathbf{t} \in \mathcal{T}$*. If* g *is supported in* $\mathbb{Z}_n^3$ *and produces the same diffraction patterns as* f *for all* $\mathbf{t} \in \mathcal{T}$*, then with probability one either*

$$g_{\mathbf{t}} = e^{\mathrm{i}\theta_0} f_{\mathbf{t}}, \quad \forall \mathbf{t} \in \mathcal{T} \tag{35}$$

or

$$g_{\mathbf{t}} = g_{\mathbf{t}'}, \quad \forall \mathbf{t}, \mathbf{t}' \in \mathcal{T}, \tag{36}$$

(including the special case $f_{\mathbf{t}} = f_{\mathbf{t}'}, \forall \mathbf{t}, \mathbf{t}' \in \mathcal{T}$*).*

Remark 5.2. *If* f *is a non-planar object than it follows that* $f_{\mathbf{t}}$ *is a non-line object for all* $\mathbf{t}$.

Remark 5.3. *With a plain (instead of random) mask, the twin-object ambiguity* $g(\mathbf{n}) = e^{\mathrm{i}\theta_0}\overline{f(-\mathbf{n})}$ *can not be eliminated.*

Proof. Suppose that, for some $\mathbf{t}_0 \in \mathcal{T}$, the first alternative in (34) holds true, i.e.

$$g_{\mathbf{t}_0}(\mathbf{n}) = e^{\mathrm{i}\theta_{\mathbf{t}_0}} f_{\mathbf{t}_0}(\mathbf{n} + \mathbf{m}_{\mathbf{t}_0})\lambda_{\mathbf{t}_0}(\mathbf{n} + \mathbf{m}_{\mathbf{t}_0}) \tag{37}$$

with

$$\lambda_{\mathbf{t}_0}(\mathbf{n}) = \mu(\mathbf{n})/\mu(\mathbf{n} - \mathbf{m}_{t_0}),$$

implying

$$\widehat{g_{\mathbf{t}_0}} = e^{\mathrm{i}\theta_{\mathbf{t}_0}} e^{\mathrm{i}2\pi \mathbf{m}_{\mathbf{t}_0}\cdot \mathbf{k}/p}\widehat{f}_{\mathbf{t}_0} \star \widehat{\lambda}_{\mathbf{t}_0}(\mathbf{k}).$$

We now prove that the second alternative in (34) can not hold. Otherwise, suppose that for some $\mathbf{t} \in \mathcal{T}$,

$$g_{\mathbf{t}}(\mathbf{n}) = e^{\mathrm{i}\theta_{\mathbf{t}}}\overline{f_{\mathbf{t}}(-\mathbf{n} + \mathbf{m}_{\mathbf{t}})\nu_{\mathbf{t}}(-\mathbf{n} + \mathbf{m}_{\mathbf{t}})} \tag{38}$$

with

$$\nu_{\mathbf{t}}(\mathbf{n}) = \mu(\mathbf{n})/\overline{\mu(-\mathbf{n} + \mathbf{m}_t)}.$$

implying

$$\widehat{g}_{\mathbf{t}}(\mathbf{k}) = \overline{\widehat{f}_{\mathbf{t}} \star \widehat{\nu}_{\mathbf{t}}(\mathbf{k})} e^{-\mathrm{i}2\pi \mathbf{m}_{\mathbf{t}}\cdot\mathbf{k}/p}$$

where $\star$ denotes the discrete convolution over the periodic grid $\mathbb{Z}_p^2$.

Let $P_{\mathbf{t}}$ denote the origin-containing (continuous) plane orthogonal to $\mathbf{t}$ in the Fourier space. By Fourier slice theorem, for all $\mathbf{k} \in P_{\mathbf{t}} \cap P_{\mathbf{t}_0}$, $\widehat{g}_{\mathbf{t}_0}(\mathbf{k}) = \widehat{g}_{\mathbf{t}}(\mathbf{k})$ and hence

$$e^{\mathrm{i}\theta_{\mathbf{t}_0}} e^{\mathrm{i}2\pi \mathbf{m}_{\mathbf{t}_0}\cdot\mathbf{k}/p}\widehat{f}_{\mathbf{t}_0} \star \widehat{\lambda}_{\mathbf{t}_0}(\mathbf{k}) = e^{\mathrm{i}\theta_{\mathbf{t}}} e^{-\mathrm{i}2\pi\mathbf{m}_{\mathbf{t}}\cdot\mathbf{k}/p}\overline{\widehat{f}_{\mathbf{t}} \star \widehat{\nu}_{\mathbf{t}}}(\mathbf{k}), \quad \forall \mathbf{k} \in P_{\mathbf{t}} \cap P_{\mathbf{t}_0}$$

implying

$$\begin{aligned} & e^{\mathrm{i}\theta_{\mathbf{t}_0}} e^{\mathrm{i}2\pi\mathbf{m}_{\mathbf{t}_0}\cdot\mathbf{k}/p} \sum_{\mathbf{n}\in\mathbb{Z}_n^2} e^{\mathrm{i}\phi(\mathbf{n})} e^{-\mathrm{i}\phi(\mathbf{n}-\mathbf{m}_{\mathbf{t}_0})} f_{\mathbf{t}_0}(\mathbf{n}) e^{-\mathrm{i}2\pi\mathbf{n}\cdot\mathbf{k}/p} \\ = \; & e^{\mathrm{i}\theta_{\mathbf{t}}} e^{-\mathrm{i}2\pi\mathbf{m}_{\mathbf{t}}\cdot\mathbf{k}/p} \sum_{\mathbf{n}\in\mathbb{Z}_n^2} e^{-\mathrm{i}\phi(\mathbf{n})} e^{-\mathrm{i}\phi(-\mathbf{n}+\mathbf{m}_{\mathbf{t}})} \bar{f}_{\mathbf{t}}(\mathbf{n}) e^{\mathrm{i}2\pi\mathbf{n}\cdot\mathbf{k}/p}, \quad \forall \mathbf{k} \in P_{\mathbf{t}} \cap P_{\mathbf{t}_0}. \end{aligned} \tag{39}$$

We now show that eq. (39) can not hold for any $\mathbf{m}_{\mathbf{t}_0}, \mathbf{m}_{\mathbf{t}}$. Consider any $\mathbf{n}$ that $f_{\mathbf{t}_0}(\mathbf{n}) \neq 0$. Due to the statistical independence of $\phi(\cdot)$ and the sign of the phases in

$$e^{\mathrm{i}\phi(\mathbf{n})} e^{-\mathrm{i}\phi(\mathbf{n}-\mathbf{m}_{\mathbf{t}_0})} f_{\mathbf{t}_0}(\mathbf{n}) e^{-\mathrm{i}2\pi \mathbf{n}\cdot\mathbf{k}/p}, \quad e^{-\mathrm{i}\phi(\mathbf{n})} e^{-\mathrm{i}\phi(-\mathbf{n}+\mathbf{m}_{\mathbf{t}})} \bar{f}_{\mathbf{t}}(\mathbf{n}) e^{\mathrm{i}2\pi \mathbf{n}\cdot\mathbf{k}/p}$$

appearing in the summation on either side of (39), the phase factor $e^{\mathrm{i}\phi(\mathbf{n})}$ on the left can not be balanced without setting $\mathbf{m}_{\mathbf{t}_0} = 0$. This then implies

$$e^{\mathrm{i}\theta_{\mathbf{t}_0}} f_{\mathbf{t}_0}(\mathbf{n}) e^{-\mathrm{i}2\pi \mathbf{n}\cdot\mathbf{k}/p} = e^{\mathrm{i}\theta_{\mathbf{t}}} e^{-\mathrm{i}2\pi \mathbf{m}_{\mathbf{t}}\cdot\mathbf{k}/p} e^{-\mathrm{i}\phi(\mathbf{n})} e^{-\mathrm{i}\phi(-\mathbf{n}+\mathbf{m}_{\mathbf{t}})} \bar{f}_{\mathbf{t}}(\mathbf{n}) e^{\mathrm{i}2\pi \mathbf{n}\cdot\mathbf{k}/p}$$

which cannot hold since the left hand size is deterministic while the right hand side is random. Consequently, (38) is false almost surely, which leaves the first of (34) the only viable alternative.

If, however, $f_{\mathbf{t}_0}(\mathbf{n}) = 0$ for all $\mathbf{n}$, then the same argument implies that $f_{\mathbf{t}}(\mathbf{n}) = 0$ for all $\mathbf{n}$. Hence the first alternative of (34) still follows, i.e.

$$g_{\mathbf{t}}(\mathbf{n}) \;=\; e^{\mathrm{i}\theta_{\mathbf{t}}} f_{\mathbf{t}}(\mathbf{n}+\mathbf{m}_{\mathbf{t}}) \lambda_{\mathbf{t}}(\mathbf{n}+\mathbf{m}_{\mathbf{t}}), \quad \forall \mathbf{t} \in \mathcal{T}, \tag{40}$$

for some $\mathbf{m}_{\mathbf{t}}$.

Consider two arbitrary, distinct directions $\mathbf{t} = \mathbf{t}_1, \mathbf{t}_2 \in \mathcal{T}$. By the Fourier slice theorem,

$$e^{\mathrm{i}\theta_{\mathbf{t}_1}} e^{\mathrm{i}2\pi \mathbf{m}_{\mathbf{t}_1}\cdot\mathbf{k}} \widehat{f}_{\mathbf{t}_1} \star \widehat{\lambda}_{\mathbf{t}_1}(\mathbf{k}) \;=\; e^{\mathrm{i}\theta_{\mathbf{t}_2}} e^{\mathrm{i}2\pi \mathbf{m}_{\mathbf{t}_2}\cdot\mathbf{k}} \widehat{f}_{\mathbf{t}_2} \star \widehat{\lambda}_{\mathbf{t}_2}(\mathbf{k}), \quad \forall \mathbf{k} \in P_{\mathbf{t}_1} \cap P_{\mathbf{t}_2} \tag{41}$$

implying

$$\begin{aligned} & e^{\mathrm{i}\theta_{\mathbf{t}_1}} e^{\mathrm{i}2\pi \mathbf{m}_{\mathbf{t}_1}\cdot\mathbf{k}/p} \sum_{\mathbf{n}\in\mathbb{Z}_n^2} e^{\mathrm{i}\phi(\mathbf{n})} e^{-\mathrm{i}\phi(\mathbf{n}-\mathbf{m}_{\mathbf{t}_1})} f_{\mathbf{t}_1}(\mathbf{n}) e^{-\mathrm{i}2\pi \mathbf{n}\cdot\mathbf{k}/p} \\ = \; & e^{\mathrm{i}\theta_{\mathbf{t}_2}} e^{\mathrm{i}2\pi \mathbf{m}_{\mathbf{t}_2}\cdot\mathbf{k}/p} \sum_{\mathbf{n}\in\mathbb{Z}_n^2} e^{\mathrm{i}\phi(\mathbf{n})} e^{-\mathrm{i}\phi(\mathbf{n}-\mathbf{m}_{\mathbf{t}_2})} f_{\mathbf{t}_2}(\mathbf{n}) e^{-\mathrm{i}2\pi \mathbf{n}\cdot\mathbf{k}/p}, \quad \forall \mathbf{k} \in P_{\mathbf{t}_1} \cap P_{\mathbf{t}_2}. \end{aligned} \tag{42}$$

Due to the statistical independence of $\phi(\cdot)$, the randomness on the both sides of (42) can not balance out unless

$$\mathbf{m}_{\mathbf{t}_1} \;=\; \mathbf{m}_{\mathbf{t}_2} (= \mathbf{m}_0) \tag{43}$$

$$\lambda_{\mathbf{t}_1} \;=\; \lambda_{\mathbf{t}_2}. \tag{44}$$

Eq. (44) means independence of $\lambda_{\mathbf{t}}$ from $\mathbf{t} \in \mathcal{T}$ and justifies the simplified notation

$$\lambda_{\mathbf{t}}(\mathbf{n}) = \lambda_0(\mathbf{n}) := \mu(\mathbf{n})/\mu(\mathbf{n}-\mathbf{m}_0) \quad \text{for some } \mathbf{m}_0 \in \mathbb{Z}^2 \text{ and all } \mathbf{t} \in \mathcal{T}. \tag{45}$$

With this, (42) reduces to

$$e^{\mathrm{i}\theta_{\mathbf{t}_1}} \sum_{\mathbf{n}\in\mathbb{Z}_n^2} e^{\mathrm{i}\phi(\mathbf{n})} e^{-\mathrm{i}\phi(\mathbf{n}-\mathbf{m}_0)} f_{\mathbf{t}_1}(\mathbf{n}) e^{-\mathrm{i}2\pi \mathbf{n}\cdot\mathbf{k}/p} \;=\; e^{\mathrm{i}\theta_{\mathbf{t}_2}} \sum_{\mathbf{n}\in\mathbb{Z}_n^2} e^{\mathrm{i}\phi(\mathbf{n})} e^{-\mathrm{i}\phi(\mathbf{n}-\mathbf{m}_0)} f_{\mathbf{t}_2}(\mathbf{n}) e^{-\mathrm{i}2\pi \mathbf{n}\cdot\mathbf{k}/p}, \tag{46}$$

for all $\mathbf{k} \in P_{\mathbf{t}_1} \cap P_{\mathbf{t}_2}$.

The function λ_0 defined in (45) is either 1 (if $\mathbf{m}_0 = 0$) or random (if $\mathbf{m}_0 \neq 0$). If $\mathbf{m}_0 = 0$, then, by (40), $g_{\mathbf{t}} = e^{\mathrm{i}\theta_{\mathbf{t}}} f_{\mathbf{t}}$ for all $\mathbf{t} \in \mathcal{T}$. By Fourier slice Theorem,

$$\begin{aligned} \widehat{f}_{\mathbf{t}}(\mathbf{k}) &= \widehat{f}_{\mathbf{t}_0}(\mathbf{k}), \quad \forall \mathbf{k} \in P_{\mathbf{t}} \cap P_{\mathbf{t}_0} \\ \widehat{g}_{\mathbf{t}}(\mathbf{k}) &= \widehat{g}_{\mathbf{t}_0}(\mathbf{k}), \quad \forall \mathbf{k} \in P_{\mathbf{t}} \cap P_{\mathbf{t}_0} \end{aligned}$$

and hence $\theta_{\mathbf{t}} = \theta_0$ for some $\theta_0 \in \mathbb{R}$ and all $\mathbf{t} \in \mathcal{T}$. In other words, $g_{\mathbf{t}} = e^{\mathrm{i}\theta_0} f_{\mathbf{t}}, \forall \mathbf{t} \in \mathcal{T}$.

If $\mathbf{m}_0 \neq 0$, then (46) and the statistical independence of $\phi(\cdot)$ imply that

$$e^{\mathrm{i}\theta_{\mathbf{t}_1}} \widehat{f}_{\mathbf{t_1}} = e^{\mathrm{i}\theta_{\mathbf{t}_2}} \widehat{f}_{\mathbf{t_2}}, \quad \forall \mathbf{t}_1, \mathbf{t}_2 \in \mathcal{T}. \tag{47}$$

Hence by (40) and (43)

$$g_{\mathbf{t_1}} = g_{\mathbf{t_2}}, \quad \forall \mathbf{t}_1, \mathbf{t}_2 \in \mathcal{T},$$

almost surely. In other words, $g_{\mathbf{t}}$ is independent of $\mathbf{t} \in \mathcal{T}$ with probability one.

Let us turn to the remaining undesirable alternative:

$$g_{\mathbf{t}}(\mathbf{n})\mu(\mathbf{n}) = e^{\mathrm{i}\theta_{\mathbf{t}}} \overline{f_{\mathbf{t}}(-\mathbf{n} + \mathbf{m_t})\mu(-\mathbf{n} + \mathbf{m_t})}, \quad \forall \mathbf{t} \in \mathcal{T} \tag{48}$$

or, equivalently, (38).

For two distinct projections $\mathbf{t} = \mathbf{t}_1, \mathbf{t}_2 \in \mathcal{T}$, (38) implies

$$e^{-\mathrm{i}\theta_{\mathbf{t}_1}} \widehat{f}_{\mathbf{t}_1} \star \widehat{\nu}_{\mathbf{t}_1}(\mathbf{k}) = e^{-\mathrm{i}\theta_{\mathbf{t}_2}} \widehat{f}_{\mathbf{t}_2} \star \widehat{\nu}_{\mathbf{t}_2}(\mathbf{k}), \quad \forall \mathbf{k} \in \mathcal{P}_{\mathbf{t}_1} \cap \mathcal{P}_{\mathbf{t}_2}. \tag{49}$$

which, at $\mathbf{k} = 0$, means

$$e^{-\mathrm{i}\theta_{\mathbf{t}_1}} \sum_{j,k \in \mathbb{Z}_n} \widehat{f}_{\mathbf{t_1}}(j,k) \widehat{\nu_{\mathbf{t}_1}}(-j,-k) = e^{-\mathrm{i}\theta_{\mathbf{t}_1}} \sum_{j,k \in \mathbb{Z}_n} \widehat{f}_{\mathbf{t_2}}(j,k) \widehat{\nu_{\mathbf{t}_2}}(-j,-k).$$

The rest of the argument follows exactly the same pattern as that following (46).

□

In view of Theorem 5.1, with a randomly coded aperture, the uniqueness problem of phase retrieval is only slightly more difficult than that of computed tomography, with only the additional ambiguity (36) to resolve.

First let us digress and consider some generic schemes that guarantee uniqueness for computed tomography.

Example 5.4. Let $\mathcal{T}$ consist of the projections represented as (20):

$$\mathcal{T} = \{(\alpha_l, \beta_l, 1) : l = 1, \ldots, m\}, \tag{50}$$

for some $m \in \mathbb{Z}$ and suppose (35) holds, i.e.

$$g_{\mathbf{t}} = e^{\mathrm{i}\theta_0} f_{\mathbf{t}}, \quad \forall \mathbf{t} \in \mathcal{T}.$$

By the Fourier slice theorem, we have

$$\widehat{g}(j,k,-\alpha_l j - \beta_l k) = e^{\mathrm{i}\theta_0} \widehat{f}(j,k,-\alpha_l j - \beta_l k), \quad l = 1, \ldots, m, \tag{51}$$

where both $\widehat{g}(j,k,\cdot)$ and $\widehat{f}(j,k,\cdot)$ are p-periodic signals bandlimited to $\pi(n-1)/p$ (for odd integer n, cf. (11)). In order to conclude that $\widehat{g} = e^{\mathrm{i}\theta_0}\widehat{f}$, it suffices to have

$$|\{\alpha_l j + \beta_l k \pmod{p} : l = 1, \ldots, m\}| \geq n, \quad \forall (j,k) \neq (0,0), \tag{52}$$

which is also a necessary condition for the validity of $\widehat{g} = e^{\mathrm{i}\theta_0}\widehat{f}$, in general (see [20]).

Slightly modifying the observation in Example 5.4, we can state the following uniqueness theorem for 3D discrete computed tomography.

Theorem 5.5 (Uniqueness of CT). *Let $\mathcal{T}$ be* **any** *one of the following three sets of projections:*

$$\begin{array}{ll} (x) & \{(1, \alpha_l, \beta_l) : l = 1, \ldots, m\} \\ (y) & \{(\alpha_l, 1, \beta_l) : l = 1, \ldots, m\} \\ (z) & \{(\alpha_l, \beta_l, 1) : l = 1, \ldots, m\}. \end{array}$$

Then $g = e^{i\theta_0} f$, whenever $g_{\mathbf{t}} = e^{i\theta_0} f_{\mathbf{t}}$ for all $\mathbf{t} \in \mathcal{T}$ and some constant $\theta_0 \in \mathbb{R}$, if and only if the condition (52) *holds true.*

Remark 5.6. *The condition* (52) *can be achieved with overwhelming probability by randomly and independently selecting n pairs of (α_l, β_l) (i.e. $m = n$) with the uniform distribution over the square $|\alpha_l|, |\beta_l| < 1$, [3].*

In view of the Fourier slice theorem, the redundancy in 3D discrete CT due to the overlap of Fourier planes with different normal vectors (i.e. the common lines) can be roughly estimated as follows. Every pair of Fourier planes share a common line of about n degrees of freedom. There are in general $n(n-1)/2$ pairs from n distinct Fourier planes and hence $n^2(n-1)/2$ degrees of information overlap. As oversampling the projection planes (cf. (27) *&* (28)*) compensates the information overlap, n generic projections contain sufficient information for determining the n^3 degrees of freedom in the object.*

In X-ray diffractive imaging, a most commonly used scheme is rotated projections about an axis orthogonal to the directions of projection. For example,

$$\{(\alpha_l, 0, 1) : l = 1, \ldots, m\},$$

where α_l are distinct numbers, represents a sequence of projections rotated about the y-axis. More generally, rotated projections forming the same angle $\arctan(\gamma)$ with, say, the z-axis, can be represented as

$$\{(\gamma \cos t_j, \gamma \sin t_j, 1) : j = 1, \ldots, m\}.$$

Next, we demonstrate that with one additional projection to the scheme such as in Example 5.4, one can eliminate the possibility (36) and resolve the uniqueness problem for tomographic phase retrieval.

Example 5.7 (Resolution of ambiguity (36)). Let $\mathcal{T}$ consist of the projections represented as (18):

$$\mathcal{T} \;=\; \{(1, \alpha_l, \beta_l) : l = 1, \ldots, n\} \cup \{(0, \alpha_0, \beta_0)\}$$

satisfying (52) and $(\alpha_0, \beta_0) \neq (0, 0)$.

In terms of the X-ray transform, (36) means that, for some $c(\cdot, \cdot)$ independent of α, β,

$$\widehat{g}_{x(\alpha,\beta)}(j, k) \;=\; c(j, k) \tag{53}$$

and hence by Fourier Slice Theorem

$$\widehat{g}(-\alpha j - \beta k, j, k) \;=\; c(j, k) \tag{54}$$

for $j, k \in \mathbb{Z}_p$.

Let

$$\widehat{g}(\xi,\eta,\zeta) = \sum_m \widehat{g}_{\eta\zeta}(m) e^{-2\pi \mathrm{i} m\xi/p} \tag{55}$$

with

$$\widehat{g}_{\eta\zeta}(m) \;=\; \sum_l \widehat{g}_\eta(m,l) e^{-2\pi \mathrm{i} l\zeta/p} \tag{56}$$

and

$$\widehat{g}_\eta(m,l) \;=\; \sum_k g(m,k,l) e^{-2\pi \mathrm{i} k\eta/p}. \tag{57}$$

By the support constraint $\mathrm{supp}(g) \in \mathbb{Z}_n^3$, (55) becomes the $n \times n$ Vandermonde system

$$V\widehat{g}_{\eta\zeta} = \begin{bmatrix} c(\eta,\zeta) \\ c(\eta,\zeta) \\ \vdots \\ c(\eta,\zeta) \end{bmatrix}. \tag{58}$$

with

$$V \;=\; [V_{ij}], \quad V_{ij} = e^{-2\pi \mathrm{i}\xi_i j/p}, \quad \xi_i = -\alpha_i\eta - \beta_i\zeta. \tag{59}$$

which is nonsingular if and only if $\{\xi_i : i = 1,\ldots,n\}$ has n distinct members.

Since the system (58) has a unique solution for $(\eta,\zeta) \neq (0,0)$, we identify $\widehat{g}_{\eta\zeta}(\cdot)$ to be the discrete δ-function located at 0 with amplitude $c(\eta,\zeta)$ for $(\eta,\zeta) \neq (0,0)$.

For $\eta, m \neq 0$, $\widehat{g}_{\eta\zeta}(m) = 0$ for all ζ and hence $\widehat{g}_\eta(m,l) = 0$ for all l. Likewise for (57), we select n distinct, nonzero values for η to perform inversion of the Vandermonde system and obtain

$$g(m,k,l) = 0, \quad m \neq 0. \tag{60}$$

In other words, g is supported on the $y - z$ plane. Consequently the projection in the direction of $(0,\alpha_0,\beta_0)$ of g would be a line object, contradicting to the assumption of non-line projection in Theorem 5.1. Therefore, (36) is false and (35) holds true almost surely for the scheme $\mathcal{T}$ under the assumptions of Theorem 5.1.

Slightly extending the above analysis, we are ready to state the final result.

Theorem 5.8. *Let $\mathcal{T}$ be* **any** *one of the following three sets of projections:*

$$\begin{array}{ll} (x') & \{(1,\alpha_l,\beta_l) : l = 1,\ldots,n\} \cup \{(0,\alpha_0,\beta_0)\} \\ (y') & \{(\alpha_l,1,\beta_l) : l = 1,\ldots,n\} \cup \{(\alpha_0,0,\beta_0)\} \\ (z') & \{(\alpha_l,\beta_l,1) : l = 1,\ldots,n\} \cup \{(\alpha_0,\beta_0,0)\} \end{array}$$

satisfying condition (52) *(with $m = n$) and* $(\alpha_0,\beta_0) \neq (0,0)$. *Then under the assumptions of Theorem 5.1, we have $g = e^{\mathrm{i}\theta_0} f$, for some constant $\theta_0 \in \mathbb{R}$, with probability one.*

6. Conclusion and discussions

The key to our approach is Theorem 5.1 which essentially reduces 3D discrete tomographic phase retrieval to computed tomography (CT).

Uniqueness condition for CT (Theorem 5.5) sets a lower bound n on the number of diffraction patterns needed for tomographic phase retrieval since each diffraction pattern contains no more information than the corresponding projection ($f_{\mathbf{t}}$ determines the autocorrelation of $f_{\mathbf{t}}$ but not vice versa). Therefore, Theorems 5.8 is nearly, if not exactly, sharp in terms of the required number of diffraction patterns.

On the other hand, Theorem 5.8 (condition (52) in particular) defines a fairly general class of measurement schemes. A natural question is, Which one is optimal and in what sense? This will be the subject of our forthcoming study.

In realistic measurements, noise is inevitable. And because of the significant amount of oversampling (cf. (27)-(28)), independent noise in the data necessarily results in an inconsistent inverse problem, i.e. there is no object whose tomographic data coincide with the given noisy data. This is characteristic of the ill-posedness of inverse problems in general. Noise stability analysis for tomographic phase retrieval is technically challenging and currently lacking. In practice, however, noisy reconstruction can often be effectively performed by utilizing prior information and regularization such as Tikhonov regularization [18].

Other useful regularizations include sparsity-promoting priors such as ℓ_1 and total variation regularizations. In our setting, for a sparse object whose projection $f_{\mathbf{t}}$ is supported on a much smaller set than $\mathbb{Z}_p^2$, the diffraction pattern can be measured at a comparably small (up to a poly-logorithmic factor of n), randomly selected subset of $\mathbb{Z}_{2p-1}^2$ from which the autocorrelation of $f_{\mathbf{t}}$ can be recovered by ℓ_1-minimization method with the random partial Fourier matrix as the sampling matrix in (26) (see [5,24]). The total-variation regularization can be used for gradient-sparse objects [9]. Similar approaches have been implemented in 3D digital holography [16], [4].

Acknowledgments

I thank Qi Yu for helpful discussions about Example 5.7. The research is supported by the Simons Foundation grant FDN 2019-24 and the NSF grant CCF-1934568.

References

[1] A. Averbuch and Y. Shkolnisky, "3D discrete X-ray transform," *Appl. Comput. Harmon. Anal.* **17** (2004) 259-276.

[2] A. Barty, J. Küpper and H. N. Chapman, "Molecular imaging using X-ray free-electron lasers," *Annu. Rev. Phys. Chem.* **64** (2013), 415-435.

[3] R. F. Bass and K. Gröchenig, "Random sampling of bandlimited functions," *Israel J. Math* **177** (2010), 1-28.

[4] J. Birdi, S. Rajora, M. Butola and K. Khare, "True 3D reconstruction in digital holography," *J. Phys. Photonics* **2** (2020) 044004.

[5] E.J. Candès and J. Romberg, "Sparsity and incoherence in compressive sampling." *Inverse Probl.* **23(3)** (2007), 969-985.

[6] B. Chen and J. J. Stamnes, “Validity of diffraction tomography based on the first Born and the first Rytov approximations,” *Appl. Opt.* **37** (1998) 2996-3006.
[7] A. J. Devaney, *Mathematical Foundations of Imaging, Tomography and Wavefield Inversion*, Cambridge University Press, 2012.
[8] A. Fannjiang, “Absolute uniqueness of phase retrieval with random illumination,” *Inverse Problems* **28** (2012), 075008.
[9] A. Fannjiang, “ TV-min and greedy pursuit for constrained joint sparsity and application to inverse scattering,” *Math. Mech. Complex Syst.* **1** (2013), 81-104.
[10] A. Fannjiang and T. Strohmer, “ The numerics of phase retrieval,” *Acta Num.* **29** (2020), 125-228.
[11] J. Frank, *Three-Dimensional Electron Microscopy of Macromolecular Assemblies*, 2nd edition, Oxford University Press, New York, 2006.
[12] M. Gemmi, E. Mugnaioli, T. E. Gorelik, U. Kolb, L. Palatinus, P. Boullay, S. Hovmller, and J. P. Abrahams, “3D electron diffraction: The nanocrystallography revolution,” *ACS Central Science* **5** (8) (2019), 1315-1329.
[13] M. Hayes, “The reconstruction of a multidimensional sequence from the phase or magnitude of its Fourier transform,” *IEEE Trans. Acoust. Speech Signal Process.* **30** (1982), 140-154.
[14] S. Helgason, *Integral Geometry and Radon Transforms*, Springer, New York, 2011.
[15] R. Horstmeyer, J. Chung, X. Ou, G. Zheng and C. Yang, “Diffraction tomography with Fourier ptychography,” *Optica* **3(8)** (2016), 827-835.
[16] U. S. Kamilov, I. N. Papadopoulos, M. H. Shoreh, A. Goy, C. Vonesch, M. Unser and D. Psaltis, “Optical tomographic image reconstruction based on beam propagation and sparse regularization,” *IEEE Trans. Comput. Imaging* **2** (2016), 59-70.
[17] U. Leonhardt, *Measuring the Quantum State of Light*, Cambridge University Press, 1997.
[18] R. Ling, W. Tahir, H.-Y. Lin, H, Lee and L. Tian, “High-throughput intensity diffraction tomography with a computational microscope,” *Biomedical Optics Express* **9** (2018), 2130-2141.
[19] K. P. MacCabe, A. D. Holmgren, M. P. Tornai and D. J. Brady, “Snapshot 2D tomography via coded aperture x-ray scatter imaging,” *Appl. Opt.***52** (2013), 4582-4589.
[20] E. Margolis and Y.C. Eldar,“Nonuniform sampling of periodic bandlimited signals,” *IEEE Trans. Signal Processing* **56** (2008), pp. 2728-2745.
[21] F. Natterer, *The Mathematics of Computerized Tomography*, Society for Industrial and Applied Mathematics, 2001.
[22] D. M. Paganin and D. Pellicciab, “X-ray phase-contrast imaging: a broad overview of some fundamentals,” *Advances in Imaging and Electron Physics* **218** (2021) 63-158.
[23] A. Sentenac and J. Mertz, “Unified description of three-dimensional optical diffraction microscopy: from transmission microscopy to optical coherence tomography: tutorial” *J. Opt. Soc. Am.***35** (2018) 748-754.
[24] J.A. Tropp, J.N. Laska, M.F. Duarte, J.K. Romberg and R.G. Baraniuk, “Beyond Nyquist: Efficient sampling of sparse bandlimited signals.” *IEEE Trans. Inform. Theor.* **56(1)** (2010), 520-544.
[25] E. Wolf, “Three-dimensional structure determination of semi-transparent objects from holographic data,” *Opt. Commun.* **1** (1969) 153-156.
[26] E. Wolf, “Determination of the amplitude and the phase of scattered fields by holography,” *J. Opt. Soc. Am.* **60** (1970) 18-20.
[27] R. M. Young, *An Introduction to Nonharmonic Fourier Series.* New York: Academic, 1980.

DEPARTMENT OF MATHEMATICS, UNIVERSITY OF CALIFORNIA, DAVIS, CALIFORNIA 95616, USA. EMAIL: FANNJIANG@MATH.UCDAVIS.EDU